Volume 18 | Number 7 | 7 April 2016 | Pages 1821–2242

Green Chemistry

Cutting-edge research for a greener sustainable future
www.rsc.org/greenchem

ISSN 1463-9262

ROYAL SOCIETY OF CHEMISTRY

CRITICAL REVIEW
G. Chatel et al.
Heterogeneous catalytic oxidation for lignin valorization into valuable chemicals: what results? What limitations? What trends?

175 YEARS

ROYAL SOCIETY OF CHEMISTRY

rsc.li/green-chem

Green Chemistry

ARTICLE

Expedient Preparation of Active Pharmaceutical Ingredient Ketamine under Sustainable Continuous Flow Conditions

Victor-Emmanuel Kassin,[a,†] Romaric Gérardy,[a,†] Thomas Toupy,[a] Diégo Collin,[a] Elena Salvadeo,[a,b] François Toussaint,[a] Kristof Van Hecke[c] and Jean-Christophe M. Monbaliu[a,*]

A robust three-step continuous flow procedure is presented for the efficient and sustainable preparation of active pharmaceutical ingredient ketamine. The procedure relies on the main assets of continuous flow processing, starts from commercially available chemicals, utilizes low toxicity reagents and a FDA class 3 solvent under intensified conditions. The procedure features a unique hydroxylation step with molecular oxygen, a fast imination relying on triisopropyl borate and a thermolysis employing Montmorillonite K10 as a heterogeneous catalyst, all three steps being performed in ethanol. The three individual steps can be run independantly or can be concatenated, thus providing a compact yet efficient setup for the production of ketamine. The scalability of the critical hydroxylation step was assessed in a commercial pilot continuous flow reactor. The process can also be adapted for the preparation of ketamine analogs. A thorough computational study on the backbone rearrangement of the cyclopentylphenylketone scaffold under thermal stress rationnalizes the experimental selectivity and the various experimental observations reported herein.

Introduction

(±)-2-(2-Chlorophenyl)-2-(methylamino)-cyclohexanone ((±)-**1a**), also known as ketamine, belongs to a class of active pharmaceutical ingredients (APIs) derived from the parent phencyclidine scaffold (arylcyclohexylamines, Figure 1). The two enantiomers of ketamine are usually referred to as esketamine ((*S*)-**1a**) and arketamine ((*R*)-**1a**).
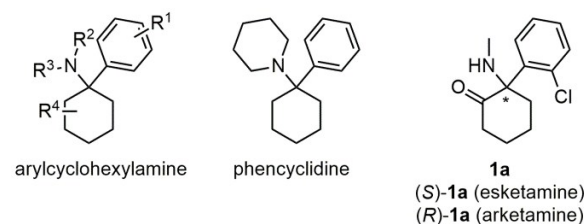

Fig. 1 General structure of the arylcyclohexylamine class of active pharmaceutical ingredients, the parent phenylcyclidine and ketamine (**1a**).

[a.] *Center for Integrated Technology and Organic Synthesis, Research Unit MolSys, University of Liège, B-4000 Liège (Sart Tilman), Belgium*
jc.monbaliu@uliege.be www.citos.uliege.be

[b.] *Alysophil SAS, 2000 Route des Lucioles Starter Business Center – CS 70337 Les Algorithmes - Bât. Thalès, 06410 Biot - Sophia Antipolis, France*

[c.] *XStruct, Department of Chemistry, Ghent University, Krijgslaan 281-S3, B-9000 Ghent, Belgium*

[†] *These authors have contributed equally to this manuscript*

Ketamine was first accepted as an ingredient for anesthetic cocktails in the late 1960s on humans and for veterinary use.[1] As a consequence of strong dissociative side effects, it was progressively withdrawn from the pharmacopeia, although it is still listed as a general anesthetic on the World Health Organization (WHO) list of essential medicines.[2] Since 1999, it is also listed as a Schedule III non-narcotic substance under the Controlled Substances Act.[3,4]

The last few years have witnessed a renewed interest for ketamine, since it is now considered a breakthrough medication for treating major depressive disorders with imminent risk for suicide.[1,5] Depression has become a major public health challenge, both at the social and economic levels according to WHO.[6] Despite the availability of various antidepressants, several weeks, if not months, are necessary to be effective on depressive patients. Ketamine, on the contrary, is effective after the first intake.[1] The Janssen Pharmaceutical Companies of Johnson & Johnson released earlier this year the results from two Phase III clinical studies emphasizing the significant and rapid reduction of depressive symptoms while using (*S*)-**1a** as a nasal spray formulation.[7] The US Food and Drug Administration (FDA) has just accepted (March 5, 2019) this formulation as medication for treatment-resistant depression. Ketamine acts on the central nervous system as a non-competitive glutamatergic *N*-methyl-D-aspartate (NMDA) receptor antagonist. Enantiomer (*S*)-**1a** is more potent, although the pharmacology profile of ketamine is complex and not completely resolved yet.[1,8] The most common pharmaceutical formulation of ketamine still consists

ARTICLE

of an aqueous solution of the racemate as a hydrochloride salt (Ketalar, Calypsol, Vetalar).
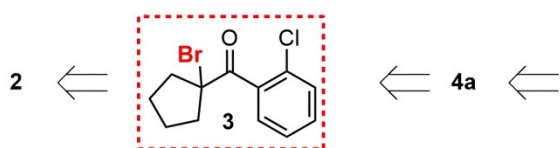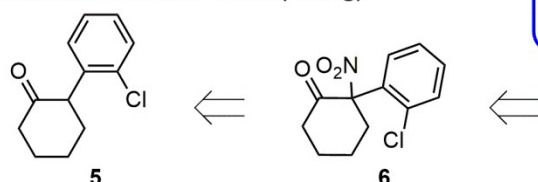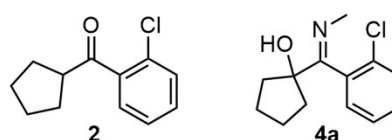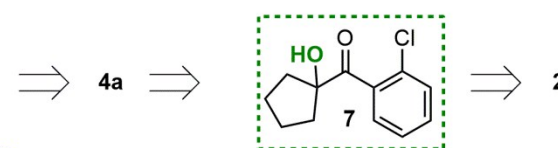
Fig. 2 Retrosynthetic strategies for the preparation of racemic ketamine, (±)-**1a** and its hydrochloride (±)-**1a**·HCl.

The pioneering work that eventually led to the preparation of racemic ketamine ((±)-**1a**) was reported in the early 1960s by Stevens in a series of papers describing the complex behavior of α-hydroxy imines and isomeric α-amino ketones under thermal stress (Figure 2a).[9–15] Stevens' procedure involved a bromination-imination-thermolysis sequence and was adopted in the recent literature for the preparation of libraries of ketamine analogs. [1,16–18]

The bromination step on an advanced ketone intermediate (**2**) toward **3** is typically wasteful and involves *N*-bromosuccinimide/benzoyl peroxide, bromine or copper bromide in class I or II solvents such as carbon tetrachloride or dichloromethane. The next step usually involves the reaction of brominated intermediate **3** with pure methylamine in large excess, leading to hydroxyimine **4a**. During the last step, hydroxyimine **4a** is thermolyzed at ~ 180 °C in refluxing decalin or in refluxing dichlorobenzene for 20-120 min, preferably in the presence of hydrochloric acid. More recently, a copper-assisted method utilizing ceric ammonium nitrate $((NH_4)_2Ce(NO_3)_6)$ in excess for the direct nitration of cyclic ketones was reported by Zhang *et al.*,[19] and the method was amenable for the preparation of (±)-**1a**, with an overall isolated yield of 25% (3 steps, Figure 2b). The key nitration was carried out on ketone **5** in dichloroethane at 80 °C for 12 h, and the corresponding nitroketone **6** was next subjected to further cosmetic steps including nitro reduction and reductive amination.

The 3-4 fold higher potency of (*S*)-**1a** stimulated the development of enantioselective strategies. For instance, Kiyooka et al. reported in 2009 an asymmetric synthesis of (*S*)-**1** according to 10 steps in 21% overall yield (99% ee) and low atom economy.[20] More recently, Toste et al. reported a procedure for the direct asymmetric electrophilic amination of α-substituted ketones with di-*tert*-butyl azodicarboxylates.[21] The electrophilic amination step itself required 40-60 h at 45

°C and relied on a complex chiral organophosphoric acid catalyst, the preparation of which required several steps. The procedure was successfully applied to an advanced ketone intermediate for the preparation of (*S*)-**1a**, which was obtained in 30% yield (99% ee) over three steps. As mentioned earlier, (±)-**1a**·HCl is a very common pharmaceutical formulation; (*S*)-**1a** can nevertheless be obtained by resolution of the racemate with (L)-(+)-tartaric acid[22] or (L)-pyroglutamic acid.[17]

It is now well established that the assets of continuous flow micro/mesofluidic reactors can be exploited to enhance global chemical performance and to drastically reduce the overall footprint of a given process.[23,24] Although transposing chemical reactions under flow conditions is not a sufficient condition to ensure sustainability, the combination of a carefully (re)designed process and the unique assets of continuous flow reactors can contribute to reduce the global environmental impact while boosting productivity.

We describe herein the development of a continuous flow process for the production of racemic ketamine. Building up on the unique, yet capricious, reactivity profile of the cyclopentylphenylketone scaffold, we revisit Stevens' classical procedure for the preparation of ketamine, and propose an economically and environmentally favorable alternative that bypasses problematic steps or conditions (Figure 2). The process utilizes exclusively low toxicity reagents and a FDA class 3 solvent under intensified conditions that minimize waste products. This procedure features 3 robust steps starting from an advanced, readily available ketone precursor **2**, and enables the atom-economic preparation of active pharmaceutical ingredient (±)-**1a** and analogs, such as norketamine (±)-**1b** and *N*-benzyl norketamine (±)-**1c**. Each step can be run individually, or can be concatenated within a single uninterrupted reactor network upon some adjustments in feed concentration and temperature. This work also reports for the first time a computational study on the backbone

rearrangement of the cyclopentylphenylketone scaffold under thermal stress, and the results rationalize the selectivity and the different experimental observations reported herein.

Experimental section

General information

Conversion and yield were determined by high performance liquid chromatography coupled to Diode-Array Detection (HPLC/DAD) or by high field ^1H NMR spectroscopy. Selectivity is defined as the ratio between the yield and the conversion. Structural identity was confirmed by ^1H and ^{13}C NMR spectroscopy (400 MHz Bruker Avance spectrometer) in CDCl₃ (Supporting Information) and by X-ray diffraction on single crystals of compounds **iso-7**, **4a** and (±)-**1a**. The chemical shifts are reported in ppm relative to TMS as internal standard or to solvent residual peak. Solvents were used as received, unless otherwise stated. Magnesium, cyclopentylbromide, 2-chlorobenzonitrile, 2-chlorophenyl cyclopentyl ketone, triethylphosphite, 1,4,7,10,13,16-hexaoxacyclooctadecane (18-C-6), 1,4,7,10,13-pentaoxacyclopentadecane (15-C-5), 1,4,7,10-tetraoxacyclododecane (12-C-4), poly(ethylene glycol) (average M_w 400, PEG-400), ethylene glycol, glycerol, triethylamine, 1,8-diazabicyclo(5.4.0)undec-7-ene (DBU), 2-*tert*-butyl-1,1,3,3-tetramethylguanidine (Barton's base), 2,8,9-trimethyl-2,5,8,9-tetraaza-1-phosphabicyclo[3.3.3]undecane (Verkade's base), 2-*tert*-butylimino-2-diethylamino-1,3-dimethylperhydro-1,3,2-diazaphosphorine (BEMP), *tert*-butylimino-tris(pyrrolidino)-phosphorane (BTPP), tetramethyl-(tris(dimethylamino)phosphoranylidene)-phosphorictriamid-ethyl-imine (P₂-Et), polystyrene-supported phosphazene base P₂-*t*-Bu, Amberlyst A26, Dowex Marathon A, Amberlite IRN 78, Ambersep 900, lithium ethoxide, sodium ethoxide, potassium ethoxide, potassium *tert*-butoxide, tetramethylammonium hydroxide (TMAOH), cesium carbonate, cesium hydroxide, sodium hydroxide, potassium hydroxide, methylamine (33 wt% in ethanol), ammonia (7 M in methanol), benzylamine, trimethyl borate, triethyl borate, triisopropylborate, titanium (IV) isopropoxide, Montmorillonite K 10, hydrochloric acid (5-6 M in isopropanol or 3 M in butanol) were obtained from commercial sources and used as received. Oxygen (Alphagaz 1) and air (Alphagaz 1) were obtained from commercial sources.

Experimental setup

Microfluidic setups. Microfluidic reactors consisted of modular continuous flow assemblies constructed with plug-and-play thermoregulated SS packed-bed column (12.5 cm × 7 mm o.d. × 4 mm i.d. or 10 cm × 13 mm o.d. × 9 mm i.d.), PFA (1.58 mm outer diameter, 800 μm internal diameter) or stainless steel (SS) coils (1.58 mm outer diameter, 500 μm internal diameter) equipped with SS connectors and ferrules (Valco) or PEEK/ETFE connectors and ferrules (IDEX/Upchurch Scientific). Feed and collection lines consisted of PFA or PEEK tubing (1.58 mm outer diameter, 750 μm internal diameter) equipped with PEEK/ETFE connectors and ferrules (IDEX/Upchurch Scientific). Liquid feeds were handled with high force Chemyx Fusion 6000

syringe pumps equipped with SS syringes and Dupont Kalrez O-rings or with HPLC pumps (ThalesNano micro HPLC). Gas feeds (O₂ or air) were handled with Bronkhorst EL FLOW Prestige mass flow controllers. The coil reactors were thermoregulated with a Heidolph MR Hei-Tec® equipped with a Pt-1000 temperature sensor, unless otherwise stated (T > 180 °C). Downstream pressure was regulated with back pressure regulators from Zaiput Flow Technologies or from IDEX/Upchurch Scientific.

Mesofluidic setup. Mesofluidic experiments (hydroxylation step) were carried out in a Corning® Advanced-Flow™ SiC G1 reactor (6 fluidic modules connected in series, 60 mL total internal volume). In some experiments, a residence time unit (PFA loop, 1/8" o.d., 40 mL internal volume) was added downstream the reactor. Feed and collection lines consisted of PFA tubing (1/4" o.d.) equipped with PFA or SS Swagelok connectors and ferrules. Liquid feeds were handled with Corning dosing lines (FUJI Technologies™ pumps), and the gas feed (oxygen) was handled with a Bronkhorst EL FLOW Prestige or EL FLOW Select mass flow controllers. The reactor was maintained at reaction temperature with a LAUDA Integral XT 280 thermostat. Downstream pressure was regulated with a back pressure regulator from Zaiput Flow Technologies.

Computational study

Computations were performed at the B3LYP/6-31+G** level of theory with the Gaussian 09 package of programs (Revision D.01).[25] Computations were run with implicit solvent (PCM, ε = 24.852 for ethanol). Stationary points were optimized with gradient techniques (tight optimization convergence). Transition states were localized using the Newton-Raphson algorithm, and the nature of the stationary points was determined by analysis of the Hessian matrix. Activation and reaction energies were obtained from the thermochemical calculations (298.15 K, 1 atm). Intrinsic reaction coordinate (IRC) calculations were performed on each transition state.

Typical runs

Continuous flow hydroxylation toward (2-chlorophenyl)(1-hydroxycyclopentyl)methanone 7 under homogeneous conditions (microfluidic setup). The pump used to deliver the solution of (2-chlorophenyl)cyclopentyl ketone (**2**, 1 M), KOH (0.5 M), PEG-400 (1 M) and P(OEt)₃ (1.1 M) in EtOH was set to 0.2 mL min⁻¹. The mass flow controller used to deliver oxygen was set to 10 mL$_n$ min⁻¹, and both streams were mixed through a PEEK T-mixer. The biphasic mixture was reacted in a PFA capillary coil (6.5 mL internal volume, estimated 5 min residence time) at 25 °C under 11 bar of counterpressure (Figure 3a). The reactor effluent was collected at steady state, diluted with water and EtOH, and analyzed by HPLC/DAD (99% conversion, 99% selectivity, see Table 1).

Continuous flow hydroxylation toward (2-chlorophenyl)(1-hydroxycyclopentyl)methanone 7 under heterogeneous conditions (microfluidic setup). The pump used to deliver the solution of (2-chlorophenyl)cyclopentyl ketone (**2**, 0.5 M) and

P(OEt)$_3$ (1 M) in EtOH was set to 0.15 mL min^{-1}. The mass flow controller used to deliver oxygen was set to 4.2 mL$_n$ min^{-1}, and both streams were mixed through a PEEK T-mixer. The biphasic reaction mixture was reacted in a packed-bed column (12.5 cm × 7 mm o.d. × 4 mm i.d.; loading material: Ambersep 900 hydroxide, 1.6 cm³) operated at 0 °C under 8.5 bar of counter-pressure (Figure 4b). The reactor effluent was collected after 60 min of equilibration, diluted with EtOH, and analyzed by HPLC/DAD (88% conversion, >99% selectivity, see Table 2).

Continuous flow hydroxylation toward (2-chlorophenyl)(1-hydroxycyclopentyl)methanone 7 under homogeneous conditions (mesofluidic setup). The solution of (2-chlorophenyl) cyclopentyl ketone (**2**, 1 M), KOH (0.5 M), PEG-400 (1 M) and P(OEt)$_3$ (1.1 M) in EtOH was injected at a flow rate of 5 mL min^{-1} and oxygen was delivered at a flow rate of 0.125 L$_n$ min^{-1}. The two streams were mixed and reacted in a Corning® Advanced-Flow™ G1 SiC Reactor (60 mL internal volume) operated at 40 °C under 11 bar of counterpressure. The reactor effluent was sampled at steady state and analysed by HPLC/DAD (85% conversion, 95% selectivity.

Continuous flow imination toward 1-((2-chlorophenyl)(methylimino)methyl)cyclopentanol (4a) (microfluidic setup). The syringe pump used to deliver the neat solution of (2-chlorophenyl)(1-hydroxycyclopentyl)methanone (**7**) was set to 0.38 mL min^{-1} (1 equiv.), the syringe pump used to deliver the neat solution of triisopropyl borate was set to 0.79 mL min^{-1} (2 equiv.) and the syringe pump used to deliver the solution of methylamine (33 wt. % in EtOH) was set to 0.32 mL min^{-1} (1.5 equiv.). The three streams were mixed through a PEEK cross junction, and the homogeneous mixture was reacted in a PFA capillary coil (1.5 mL internal volume, 1 min of residence time) at 60 °C under 5.2 bar of counterpressure (Figure 7b). The reactor effluent was collected at steady state, diluted with EtOH, and analyzed by HPLC/DAD (>99% conversion and selectivity, see Table 3).

Continuous flow thermolysis toward (±)-ketamine ((±)-1a) under homogeneous conditions (microfluidic setup). The HPLC pump used to deliver the solution of 1-((2-chlorophenyl)(methylimino)methyl)cyclopentanol (**4a**, 0.42 M) in ethanol was set to 0.8 mL min^{-1}. The solution was thermolyzed in a SS coil (4 mL internal volume, 5 min of residence time) at 220 °C under 35 bar of counter-pressure (Figure 9a). The reactor effluent was was collected at steady state, diluted with EtOH and analyzed by HPLC/DAD (71% conversion, 78% selectivity, see Table 4).

Continuous flow thermolysis toward (±)-ketamine ((±)-1a) under heterogeneous conditions (microfluidic setup). The HPLC pump used to deliver the solution of 1-((2-chlorophenyl)(methylimino)methyl)cyclopentanol (**4a**, 0.42 M) in ethanol was set to 0.8 mL min^{-1}. The solution was preheated in a SS loop (0.5 mL internal volume), and reacted in a SS packed-bed column (10 cm × 13 mm o.d. × 9 mm i.d., packing

material: 3.7 g of Montmorillonite K10 in granules) at 180 °C under 35 bar of counter-pressure (Figure 9.b). After 60 min of operation, the reactor effluent was collected, diluted with EtOH and analyzed by HPLC/DAD (69% conversion, 89% selectivity, see Table 6). Concentration of the reactor effluent and cooling to -18 °C afforded crystals of (±)-**1a** free base. (36% isolated yield, 99% purity). Alternatively, addition of 2 volumes of HCl (1 M in diethyl ether) gave selective precipitation of **1a**·HCl (62% isolated yield, 99% purity).

Concatenated process toward (±)-ketamine ((±)-1a), (±)-norketamine ((±)-1b) and (±)-N-benzylnorketamine ((±)-1c). The feed solution of (2-chlorophenyl) cyclopentyl ketone (**2**, 1 M), KOH (0.5 M), PEG-400 (0.5 M) and P(OEt)$_3$ (1.1 M) in EtOH was injected at a flow rate of 0.25 mL min^{-1} and reacted with oxygen (10 mL$_n$ min^{-1}) at 25 °C for 5 min of residence time (11 bar). The reactor effluent was next mixed with a neat solution of triisopropyl borate (0.13 mL min^{-1}, 2 equiv.) and with Feed solution 2 (option a: MeNH$_2$, 33 wt. % in EtOH, 0.05 mL min^{-1}; option b: NH$_3$ 7 M in MeOH, 0.29 mL min^{-1}; option c: neat benzylamine, 0.04 mL min^{-1}). The three streams were mixed through a PEEK cross junction, and the homogeneous mixture was reacted in a PFA coil at 25 °C for 2 min of residence time (7 bar). The reactor effluent containing either **4a** (option a), **4b** (option b) or **4c** (option c) was diluted with EtOH and analyzed by HPLC/DAD (option a: conv. (**2**) = 98%, selec. = 95%; option b: conv. (**2**) = 55%, selec. = 98%; option c: conv. (**2**) = 99%, selec. = 99%). The hydroxylation-imination reactor effluent was collected in a surge, diluted with ethanol (0.02 M in **4a-c**) and reinjected at a flow rate of 1.6 mL min^{-1}. The solution was preheated in a SS loop (0.5 mL internal volume), and reacted in a SS packed-bed column (10 cm × 13 mm o.d. × 9 mm i.d., packing material: 3.7 g of Montmorillonite K10 in granules) at 180 °C under 35 bar of counter-pressure (see Figure 11). After 20 min of operation, the effluent of the reactor was collected, diluted with EtOH, and analyzed by HPLC/DAD ((±)-**1a**: conv. (**4a**) = 70%, selec. 93%; (±)-**1b**: conv. (**4b**) = 99%, selec. 99% or (±)-**1c**: conv. (**4b**) = 60%, selec. 81%).

Results and Discussion

Hydroxylation of ketone 2 under microfluidic conditions

While considering alternatives for designing an effective flow process for the preparation of (±)-**1a**, hydroxyketone **7** rapidly emerged as a robust alternative to bromoketone **3**, which is a pivotal intermediate in Stevens' original procedure. Bromoketone **3** is readily available from ketone **2**, but its preparation is wasteful. Since ketone **2** is commercially available, but can also be synthesized from cheap and widely available chemicals (Supporting Information, section 2.2.1), we decided to keep **2** as starting material.

A wide variety of methods for the preparation of tertiary α-hydroxycarbonyl compounds directly from ketones or analogs has been reported so far, although many procedures require either the use of transition metal catalysts or environmentally harmful chemicals. Among these procedures, several

ARTICLE

considered the direct use of molecular oxygen as a primary oxidizer, which is very appealing given its wide availability and low toxicity profile.[26] For instance, Jiao reported a hydroxylation procedure using molecular oxygen in the presence of a basic catalyst (20 mol% Cs_2CO_3) and a reductant ($P(OEt)_3$) in DMSO.[27] An enantioselective approach involving molecular oxygen, aqueous NaOH, a chiral phase transfer catalyst and a reductant ($P(OEt)_3$ or dppe) in benzene was reported by Zhao.[28] A few years later, Gnanaprakasam reported an alternative hydroxylation procedure in the presence of air and a stoichiometric base (*t*BuOK) in DMSO or toluene, in the absence of an external reductant.[29] Jiao's procedure was applied in batch to ketone **2**, providing compound **7** in high yield and selectivity after 3 h on a 1 g scale in DMSO. On a 40 g scale, about 10 h were required to reach completion. The procedure was difficult to scale-up in batch, mostly due to a high exotherm and the poor mass transfer between oxygen and the liquid phase, giving inconsistent results. Further optimization, including the use of ethanol as a solvent, led to longer reaction times (up to 24 h) to reach a similar conversion. As is, the conditions were not directly transposable to flow, and a solution was sought.

DMSO is a FDA class 3 solvent, but it is listed as problematic for large scale applications by CHEM21, GSK and Sanofi solvent guides.[30–33] According to the same solvent selection guides, ethanol is considered as a green solvent, and is therefore recommended for lab and pilot scale applications. In addition, ethanol is also a FDA class 3 solvent and is compatible with the entire reaction sequence, thus potentially enabling direct telescoping without intermediate solvent swap or other operations that would negatively affect the overall process footprint. A preliminary set of conditions was screened for the hydroxylation of **2** in ethanol.

Ketone **2** has a good solubility in ethanol (up to 1 M), the limiting factor becoming the base additive. Oxygen was selected as the primary oxidizer, and homogeneous bases were screened. Unlike the conditions reported by Gnanaprakasam,[29] the presence of an external reductant was mandatory since the reaction proceeds through the formation of an intermediate hydroperoxide **per-7** that needs to be reduced . There are several reductants that can be used to convert the intermediate hydroperoxide **per-7** to hydroxyketone **7** such as phosphines,[27,28] thiourea,[34] or inorganic reductants such as sodium thiosulfate,[35] although only an ethanol-soluble reductant was eligible for this continuous flow application. Triethylphosphite is a low cost, widely available liquid reductant with a high solubility in ethanol, and is likely the least toxic reductant suitable for this application.[36] In addition, its oxidation product, *i.e.* triethyl phosphate, is also highly soluble in ethanol and has a low toxicity profile. In addition to the aforementioned, triethylphosphite and the corresponding phosphate were found unreactive under the conditions of steps 2-3, and could stay in the reactor effluent, hence avoiding wasteful intermediate purifications.

The optimization was complex due to the capricious nature of **7** that is prone to a fast α-ketol rearrangement

toward isomeric **iso-7** under basic conditions. Isomeric hydroxyketone **iso-7** was isolated and characterized, with unambiguous structure determination by X-ray diffraction on a single crystal (Figure 3b).
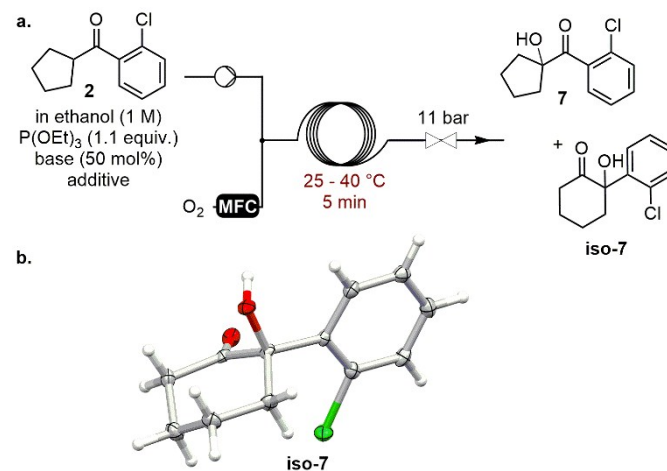

Fig. 3. a. Metal-free hydroxylation of ketone **2** with molecular oxygen under homogeneous conditions. **b.** Molecular structure by single crystal X-ray diffraction analysis of **iso-7**.

With a 1 M feedstock solution of **2** in ethanol, the optimization commenced with a thorough screening of the base additive under continuous flow conditions (Figure 3 and Table 1). The reaction was very exothermic, and the temperature of the T-mixer, where mixing of the liquid and gaseous feeds occurred, rapidly increased (actual temperature not measured). Decision was made to thermostatize the T-mixer as well as the reaction unit. A variety of commercially available organic and inorganic bases soluble in ethanol were considered (see Supporting Information, Tables S3-8 for the detailed optimization). The nature and the concentration of the base as well as the reaction temperature had a profound impact on the reaction outcome (Table 1). Cesium carbonate (0 and 20 mol%) was tested first to mimic Jiao's procedure under flow conditions (entries 1,2); however, in ethanol, only 12% conversion were observed at 25 °C within 5 min of residence time.

Non-ionic bases such as amines, amidines, guanidines and phosphazenes were selected for preliminary trials. No conversion was obtained with triethylamine (1 equiv.) or DBU, regardless of the residence time and the temperature (entries 3,4). With phosphazenes such as BTPP and P_2-Et, the conversion of **2** reached 40% and 95% (99% and 98% selectivity), respectively, at 25 °C with 50 mol% of the base (entries 5-8) within 5 min of residence time. Lower loadings of the base decreased the conversion. Increasing the temperature to 40 °C led to a slight increase for the conversion with BTPP up to 58% (99% selectivity, entry 6), while with P_2-Et, the conversion of **2** reached 99%, but the selectivity declined to 94% (entry 8). Despite the very high efficiency of phosphazene P_2-Et for the selective preparation of **7**, its cost and its impact on the global footprint of the transformation make it quite questionable for designing a sustainable approach toward ketamine (±)-**1a**.

Table 1. Process optimization for the homogeneous hydroxylation of ketone **2**

Entry[a]	Base (mol%)	Additive (mol%)	T (°C)	Conv. (%)[b]	Selec. (%)[b]
1	/	/	25	0	/
2	Cs$_2$CO$_3$ (20)	/	25	12	95
3	Et$_3$N (100)	/	25	0	/
4	DBU (100)	/	140	0	/
5	BTPP (50)	/	25	40	>99
6	BTPP (50)	/	40	58	>99
7	P$_2$-Et (50)	/	25	95	98
8	P$_2$-Et (50)	/	40	>99	94
9	LiOEt (50)	12-C-4 (50)	25	32	10
10	LiOEt (50)	12-C-4 (50)	40	40	5
11	NaOEt (50)	15-C-5 (50)	25	99	72
12	NaOEt (50)	15-C-5 (50)	40	99	54
13	KOEt (50)	18-C-6 (50)	25	>99	95
14	KOEt (50)	18-C-6 (50)	40	>99	82
15	KOtBu (100)	18-C-6 (50)	25	>99	25
16	KOtBu (50)	/	25	77	70
17	KOtBu (50)	18-C-6 (50)	25	97	98
18	KOtBu (50)	18-C-6 (50)	40	99	82
19	NaOH (50)	15-C-5 (50)	25	88	69
20	KOH (50)	/	25	85	71
21	KOH (50)	/	40	91	57
22	KOH (50)	18-C-6 (50)	25	96	97
23	KOH (50)	18-C-6 (50)	40	>99	92
24	KOH (50)	PEG-400 (50)	25	94	>99
25	KOH (50)	PEG-400 (100)	25	>99	>99
26	CsOH (50)	18-C-6 (100)	25	>99	96
27	TMAOH (50)	/	25	55	97
28	TMAOH (100)	/	25	95	95

[a] Typical conditions: [**2**] = 1 M; [P(OEt)$_3$] = 1.1 M; residence time = 5 min; P = 11 bar; liquid flow rate = 0.20 mL min^{-1}; O$_2$ flow rate = 10 mL$_n$ min^{-1}. [b] Conversion and yield were determined at steady state by HPLC/DAD processed at 220 nm.

More affordable ionic organic bases with a good solubility in ethanol were next considered. Similarly to strong non-ionic bases, the alkaline ethoxides had to be used in substoichiometric amount to maximize the selectivity toward **7**. Starting with alkaline ethoxides, both conversion and selectivity were strongly affected by the nature of the alkaline countercation (entries 9-18), and increasing conversion and selectivity were observed while increasing the softness of the countercation (Li$^+$ < Na$^+$ < K$^+$). A complex HPLC reaction profile was obtained with LiOEt. Significant improvements were obtained while adding crown ethers, and the combination of KOEt (50 mol%) and 18-crown-6 (18-C-6, 50 mol%) gave the best results with complete conversion and 95% selectivity toward **7** at 25 °C (entries 13-14). Again, the reaction was very sensitive to the temperature, and significant amounts of isomeric hydroxyketone **iso-7** were obtained at 40 °C (entries 10-18). Shifting to the more hindered KOtBu, excellent

conversion (97%) and selectivity (98%) were achieved at 25 °C in the presence of 18-C-6 (entry 17). Decreasing the residence time to 2.5 min slightly decreased the conversion to 93%, but left the selectivity unaffected.

To further improve the atom economy of the process, simple alkaline hydroxides were also assessed (entries 19-26). Sodium, potassium and cesium hydroxides were soluble in a 1 M feed solution of ketone **2** in ethanol, while lithium hydroxide was not soluble in the feed solution thus precluding reaction under flow conditions. The trend was similar to the one observed for the ethoxides. The temperature had a positive impact on the conversion, but also a deleterious effect on the selectivity, with significant amounts of isomeric **iso-7** observed at 40 °C. In the worst cases, isomeric **iso-7** crashed out from solution and clogged the reactor. Larger, softer countercations increased both the conversion and selectivity. To further confirm this observation, tetramethylammonium hydroxide (TMAOH) was also tested as a basic additive (entries 27-28), and up to 95% conversion (95% selectivity) was observed at 25 °C, although a larger amount of base was required (1:1 **2**/TMAOH ratio).

Similarly to alkaline alkoxides, the presence of the appropriate crown ethers improved both conversion and selectivity, but since crown ethers are both expensive and very toxic,[37] alternative additives were sought. The best results were obtained for potassium hydroxide in the presence of PEG-400 (entries 24-25). The hydroxylation reaction on ketone **2** reached 94% within 5 min of residence time at 25 °C in the presence of 50 mol% of KOH and PEG-400. With a (1:1 **2**/PEG-400 ratio), both conversion and selectivity toward **7** were total. The hydroxylation procedure was not directly transposable to other substrates than ketone **2** (see Supporting Information, Tables S11-12). In addition to its low toxicity profile and wide availability, PEG-400 was also found unreactive under the conditions of steps 2-3, and could stay in the reactor effluent without affecting the process. This again was seen as a major asset since it avoided wasteful intermediate purifications and enabled direct reaction telescoping. Intermediate purification of hydroxyketone **7** was however possible through column chromatography for getting analytical samples (see Supporting Information, section 2.2.2.9).

Next, the hydroxylation of **2** (1 M in ethanol) was further assessed with the optimized parameters (5 min of residence time, 25 °C, 50 mol% of KOH, 1:1 **2**/PEG-400 ratio) while changing the gas feed from industrial oxygen to air. As expected, the conversion dropped (14%) while maintaining an excellent selectivity toward **7** (98%). Increasing the temperature to 40 °C boosted the conversion to 20%, but had a deleterious impact on the selectivity (85%).

Heterogeneous bases were also considered to further increase cost-efficiency of the process and to simplify downstream processing (Table 2 and Figure 4). For the trials involving heterogeneous bases, less drastic conditions were utilized with a 0.5 M feedstock solution of **2** in ethanol and 2 equiv. of triethylphosphite. No chelating additive was required for these trials. A variety of commercially heterogenized base

ARTICLE

reagents were considered (see Supporting Information, Table S13 for the detailed optimization).

Heterogenized phosphazene such as polystyrene-supported P$_2$-t-Bu (PS-P$_2$-t-Bu) gave at best a conversion of 7% (Supporting Information, Table S13, Entry 3). The most promising results were obtained with quaternary ammonium-type anion exchange resins such as Amberlyst A26, Dowex Marathon A, Amberlite IRN 78 and Ambersep 900 (Table 2). The heterogeneous process was also strongly exothermic, and the packed-bed filled with the heterogeneous base was thermostatized. Similarly to the homogeneous process, higher temperatures had a deleterious impact on the selectivity, with increasing amounts of isomeric **iso-7** being formed**.**
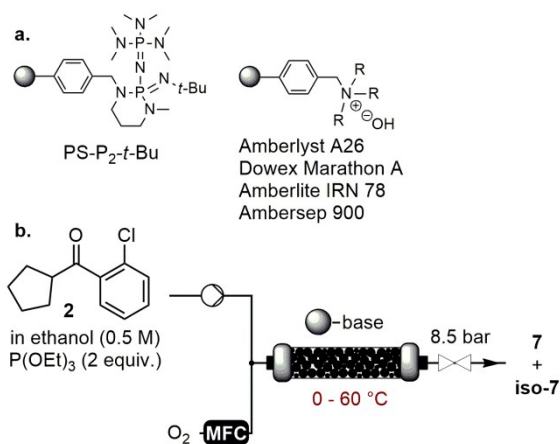

Fig. 4. a. Representative examples of heterogenized bases. **b.** Metal-free hydroxylation of ketone **2** with molecular oxygen under heterogeneous conditions

At 25 °C, Amberlyst A26 and Amberlite IRN 78 deactivated quite rapidly, while Ambersep 900 and Dowex Marathon A gave steady conversions for at least 90 min of operation (Supporting Information, Figure S11). The optimized conditions implied a packed-bed column filled with Ambersep 900 operated at 0 °C to maintain the selectivity toward compound **7** at 99%, and using a 0.15 mL min^{-1} flow rate for the liquid feed and an excess of oxygen (2.5 equiv.; 4.2 mL$_n$ min^{-1}). Under

Table 2. Process optimization for the h*e*terogeneous hydroxylation of ketone **2**.

Entry[a]	Base	T (°C)	Conv. (%)[b]	Selec. (%)[b]	STY (mol L^{-1} day^{-1})[b]
1	Amberlyst A-26	25	56	94	47.4
2	Dowex Marathon A	25	51	95	43.6
3	Amberlite IRN 78	25	46	97	40.2
4	Ambersep 900	25	64	93	53.6
5[c]	Ambersep 900	0	88	>99	59.4

[a] Typical conditions: [**2**] = 0.5 M; [P(OEt)$_3$] = 1 M; P = 8.5 bar; liquid flow rate = 0.2 mL min^{-1}; O$_2$ flow rate = 3 mL$_n$ min^{-1}, volume of the bed = 1.6 cm^3 (neat catalyst). [b] Conversion and selectivity were determined after 60 min of equilibration, by HPLC/DAD processed at 220 nm. STY = space-time yield after 60 min of equilibration. [c] Liquid flow rate = 0.15 mL min^{-1}, O$_2$ flow rate = 4.2 mL$_n$ min^{-1}.

these conditions, the conversion decreased from 95% after 30 min to 78% after 2 h of continuous operation (entry 5 and Supporting Information, Figure S13). Despite the added value of a supported base, the decrease in performance over operation time drastically reduced the practical interest.

Based upon these observations, a likely mechanism implies the formation of enolate **en-2** through the reaction of ketone **2** with base **MB**, and its reaction with molecular oxygen to form hydroperoxide anion **per-7**. Intermediate **per-7** can deprotonate in turn ketone **2** to form more of **en-2**, although ethanol is likely involved (not shown). The next step involves the reduction of hydroperoxide **per-7** with triethylphosphite to form hydroxyketone **7** (Scheme 1). Hydroperoxide **per-7** is unstable, and all attempts for isolation and characterization failed.
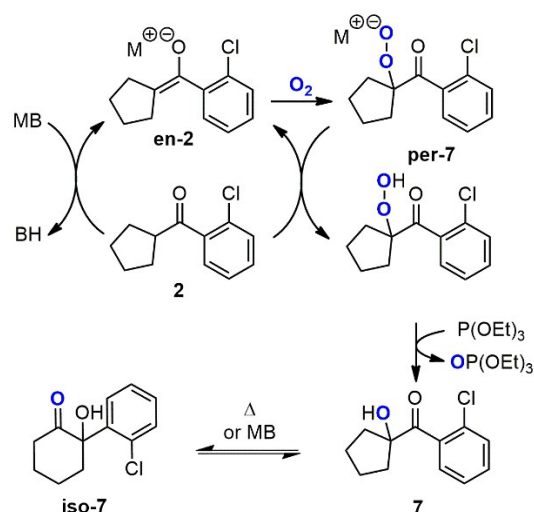
Scheme 1. Mechanism for the hydroxylation of ketone **2b** toward intermediate **7**, showing the competitive formation of isomeric hydroxyketone **iso-7**. MB is a hydroxide or alkoxide base (M is a countercation).

The results from both the homogeneous and the heterogeneous studies emphasized that the formation of isomeric hydroxyketone **iso-7** is enhanced by: (a) an excess of base, (b) the presence of hard cations and (c) heat. DFT computations on the α-ketol rearrangement of **7** to isomeric **iso-7** provided important insights in agreement with our observations and the mechanism depicted in Scheme 1. The α-ketol rearrangement proceeds through a unimolecular pseudo 3-membered ring transition state (Figure 5), and results in a profound backbone modification. Although quite common for α-hydroxyketones, the α-hydroxylcyclopentylketone is particularly sensitive to such structural rearrangement. The α-ketol rearrangement on **7** has a high activation barrier ($\Delta G^{\neq}_{neut}$ = 39.1 kcal mol^{-1}) when proceeding on neutral structures.

These values are in good agreement with experimental data collected in the 1970s by Stevens and others.[38] Under basic conditions, the activation barrier decreases significantly ($\Delta G^{\neq}_{an}$ = 11.2 kcal mol^{-1}), and thus the formation of isomeric **iso-7** becomes significant. In the presence of a hard cation (here modelled as a proton), the activation barrier for the α-

ketol rearrangement is also lower than for the neutral pathway ($\Delta G^{\ddagger}_{cat}$ = 14.6 kcal mol^{-1}). These computational results are in agreement with the mechanism in Scheme 1 and the experimental observations: a higher temperature will accelerate the α-ketol rearrangement, in particular when combined with an excess of base or a hard countercation. Excess or even stoichiometric basic reagents would negatively affect the selectivity of the reaction, and trigger the formation of isomeric hydroxyketone **iso-7**. The addition of a strong chelating agent such as a crown ether or PEG is therefore helpful to counteract the activation effect of hard cations. Further computations on the parent cyclopentylphenylketone emphasized a similar behavior ($\Delta G^{\ddagger}_{neut}$ = 38.5 kcal mol^{-1}, $\Delta G^{\ddagger}_{an}$ = 11.6 kcal mol^{-1}, $\Delta G^{\ddagger}_{cat}$ = 21.8 kcal mol^{-1}, see Supporting Information, section 3.1), thus excluding a specific effect from the ortho-chloro substituent on the phenyl group (other than decreasing the pK_a of the enolizable position in **2**). Such rearrangement was however not reported by Jiao upon the hydroxylation of cylcopentylphenyl ketone.[27]
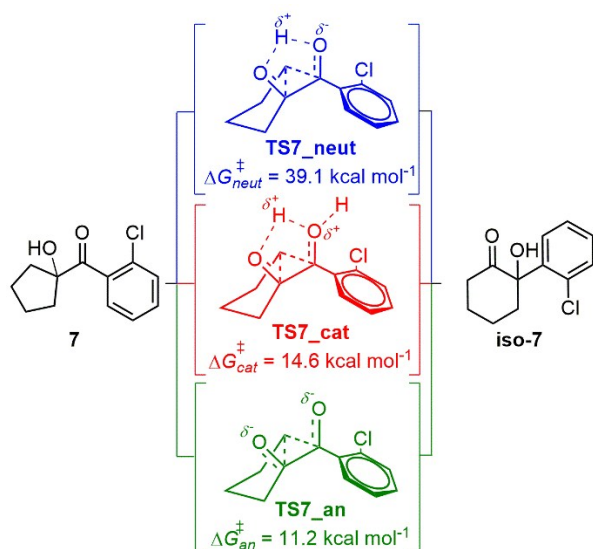

Fig. 5. Structures and Gibbs free energy ($\Delta G^{\ddagger}$) of reaction corresponding to the transition states associated with the α-ketol rearrangement of hydroxyketone **7** under basic (green, **TS7_an**), cationic (red, **TS7_cat**) and neutral (blue, **TS7_neut**) conditions. For details and cartesian coordinates, see the Supporting Information (section 3.1).

Assessment of scalability for the hydroxylation process toward hydroxyketone 7

The handling of oxygen combined with flammable organics is typically seen as a significant safety concern, especially for large scale applications. Continuous flow technology offers a safe alternative for such processes, as demonstrated by Kappe and coworkers:[26] the actual amount of reacting oxygen in the continuous flow setup per unit of time remains low, and is consumed during the course of the reaction. The excess oxygen is vented upon collection in the surge (see the description of the telescoped process) and diluted with a flow of nitrogen for direct release in the fume hood.

With the optimized microfluidic conditions for the hydroxylation of ketone **2** in hands, further scalability was

Entry[a]	[7] (M)	MeNH$_2$ (equiv.)	Additive	Residence time(min)	T (°C)	Yield (4a) (%)[b]
1	0.5	1.5	B(OiPr)$_3$	1	40	94[c]
2	0.5	1.5	B(OiPr)$_3$	1	60	>99[c]
3	neat	1.5	B(OiPr)$_3$	1	40	86
4	neat	1.5	B(OiPr)$_3$	1	60	>99[d]
5	neat	1.5	B(OiPr)$_3$	0.5	60	87

[a] Typical conditions: 2 equivalents of additive; P = 5.2 bar. [b] Yield was determined at steady state by HPLC/DAD processed at 216 nm. [c] Productivity: 65 g day^{-1}. [d] Productivity: 585 g day^{-1}.

assessed in a commercial mesofluidic silicon carbide reactor (Corning® Advanced-Flow™ G1 SiC reactor) equipped with 6 fluidic modules (Figure 6). The selection of silicon carbide rather than glass was dictated by the combination of basic conditions (KOH) and high exothermicity. The outlet of the reactor was optionally connected to a residence time unit.

The operating specifications for such reactor impose rather high flow rates for maintaining the highest mixing performance (min. 30 mL min^{-1} up to max. 200 mL total flow rate), thus leading to short residence times. For these experiments, the concentration in **2** was set at 0.5 M in ethanol with KOH (50 mol%), PEG-400 (50 mol%) and P(OEt)$_3$ (1.1 equiv.) to reduce the viscosity of the feed solution. With a 20 g min^{-1} flow rate for the liquid feed and 1 L$_n$ min^{-1} for oxygen, an estimated residence time of 30 s was obtained. We reasoned that higher temperature in conjunction with short residence time might still afford good conversion (up to 63% at 120 °C). However, as observed under microfluidic conditions, increasing the temperature also degraded the selectivity toward **7** (27%, at 120 °C) with increasing amounts of **iso-7** being formed. A selectivity of 99 % was obtained with 30 s of residence time at 40 °C (11 bar), with a conversion of 15% (daily productivity of 0.24 kg for **7**).

It rapidly appeared that a longer residence time was necessary to reach higher conversions, and decision was made to degrade the mixing efficiency and operate the reactor out of specifications (5 mL min^{-1} for the liquid feed and 125 mL$_n$ min^{-1} for the oxygen feed). Lower flow rates thus came with a longer residence time and also authorized higher feed concentration (1 M for **2** in ethanol). At 40 °C (11 bar), a conversion of 85% with a selectivity of 95% was maintained, thus corresponding to a productivity of 1.3 kg per day.
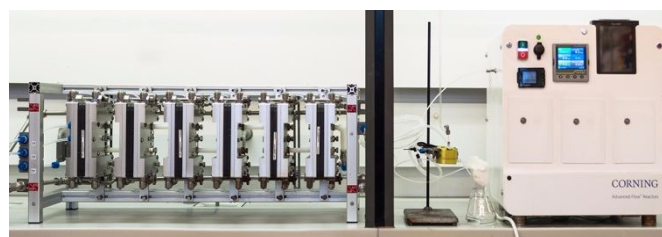

Fig. 6. Photograph of the Corning® Advanced-Flow™ G1 SiC reactor setup for the hydroxylation of ketone **2**

Imination of hydroxyketone 7 under microfluidic conditions

The imination of **7** toward the formation of hydroxyimine **4a** was next studied. Preliminary data were collected from batch experiments. The imination of **7** in ethanol with a large excess of methylamine (5 equiv.) proceeds slowly at room temperature and typically requires 3 days to reach completion (97% isolated yield). The direct transposition of these conditions under continuous flow (SS coil) was somewhat cumbersome (Figure 7a). With a solution of 0.5 M hydroxyketone **7** in ethanol, the reaction profile was clean up to 100 °C (Supporting Information, Figure S14). The conversion of hydroxyketone **7** toward **4a** reached a mere 38% (10 min of residence time). From 120 °C, ($\pm$)-**1a** could be detected in the crude reactor effluent (2%) along with unreacted **7** (43%), **4a** (53%) and other impurities. Pushing the temperature up to 180 °C did not improve further the reaction, since increasing amounts of ($\pm$)-**1a** (18%) and other side products were observed.

Based upon these preliminary observations, we looked at alternatives for increasing the conversion while maintaining the reaction time below 5 min at lower temperature. Both the results collected upon optimization of the hydroxylation of **2** and the preliminary imination trials have emphasized the emergence of competitive side-reactions upon heating the reaction mixture: above 40 °C, the amount of isomeric ketone **iso-7** becomes significant and above 160 °C the formation of ($\pm$)-**1a** already becomes noticeable.

Imine formation is typically enhanced by the use of molecular sieves, dehydration reagents and/or Lewis acids.
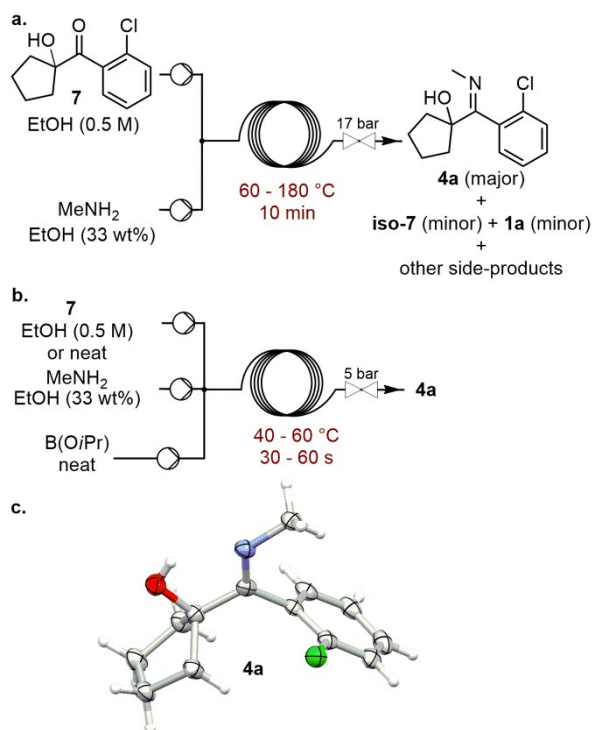

Fig. 7. a. High temperature imination of hydroxyketone **7** with methylamine. **b.** Trialkyl borate-promoted imination of hydroxyketone **7**. **c.** Molecular structure by single crystal X-ray diffraction analysis of **4a**.

Alkyl borates have received attention the last few years as low cost and low toxicity Lewis acids for various reactions, including amidation[39] and imination reactions. For instance, Reeves *et al*. reported a general imination procedure with tris(2,2,2-trifluoroethyl)borate (B(OCH$_2$-CF$_3$)$_3$).[40] To keep the process economically viable and with a low environmental impact, simple liquid trialkyl borates such as trimethyl, triethyl and triisopropyl borate were considered. Preliminary results were collected by performing reactions in HPLC vials, indicating that total conversion could be attained with only 1.5 equiv. of methylamine in the presence of 2 equivalents of B(OMe)$_3$, B(OEt)$_3$ or B(OiPr)$_3$ within 1 min of reaction time at 60 °C. These results were next validated under continuous flow conditions (Figure 7b). Three separate high pressure pumps delivered hydroxyketone **7**, MeNH$_2$ in ethanol (33 wt%) and neat triisopropyl borate, respectively. Quantitative conversion and selectivity toward the desired hydroxyimine **4a** was obtained within 1 min of residence time at 60 °C in the presence of 1.5 equiv. of methylamine and 2 equiv. of triisopropyl borate. No noticeable differences were observed between the alkyl borates. Most importantly, the conditions were amenable to crude **7** (no purification of the reactor effluent from the hydroxylation step) without impacting the conversion and the selectivity (see Supporting Information, section 2.2.6). The excess triisopropyl borate could be easily removed for getting pure hydroxyimine **4a** (see Supporting Information, section 2.2.5). However, intermediate purification was alleviated since the thermolysis step could accommodate isopropyl borate with no decrease in performance (see Table 5), hence avoiding wasteful intermediate purifications.

Similar process conditions were amenable to the preparation of hydroxyimines **4b,c**, as precursors of norketamine ($\pm$)-**1b** and *N*-benzylnorketamine ($\pm$)-**1c** (see Figure 11a), respectively. Iminols **4b,c** were obtained in good to excellent conversion and selectivity (see below and Supporting Information, section 2.2.6).

Thermolysis of iminol 4a under microfluidic conditions

The rearrangement of α-iminols, alike α-ketols, was extensively studied by Stevens[9–15,38] and described as a general phenomenon (Figure 8a) that can be triggered by thermal stress, an acid or a base.[41] Aiming at the preparation of aminoketones of type **1**, Stevens studied the rearrangement of aminoketones of type **iso-4** as well as iminols of type **4** (Figure 8b). It emphasized that the cyclopentyl fragment on **4** and derivatives was a key feature, leading upon rearrangement to a relaxed cyclohexyl backbone in high yield and selectivity; while with other acyclic substituents on the starting hydroxyimine, fragmentation or other side reactions were reported.[9–15,38] The series of papers concluded that the thermolysis of iminols of type **4** was more efficient than the thermolysis of aminoketones of type **iso-4** for producing aminoketones of type **1**. Such thermolysis was described to occur at temperatures > 180 °C without a catalyst (reaction time 2-3 h). At temperatures higher than 230 °C, the yield dropped and extensive decomposition was reported. Typical yields at 180 °C in dichlorobenzene or decane are of 70 and

ARTICLE

Journal Name

75%, respectively. Several acids were also tested for the thermal rearrangement toward **1**; in all cases, the iminol salts afforded higher yields in shorter reaction times and at lower temperature than with the free bases of type **4**. For instance, up to 95% yield was obtained upon thermolysis of **4** in the presence of HCl in dichlorobenzene. The authors also reported that the thermal rearrangement was also sensitive to solvent polarity, and swapping to more polar solvents increased the conversion. It was suggested that the presence of an acid would trigger the formation of an ammonium salt of **1**, thus allowing **1** to escape the series of interconnected equilibria.

The conclusions of Stevens' series of papers can be easily transposed for the preparation of (±)-**1a** or analogs (±)-**1b,c**, and a potential complex reaction profile is expected as a consequence of four interconnected isomeric species (Figure 8b). Several studies utilized the thermal rearrangement of iminol **4a** in the presence of HCl for the preparation of ketamine hydrochloride, as well as for the preparation of ketamine analogs and metabolites.[16,17,42,43]
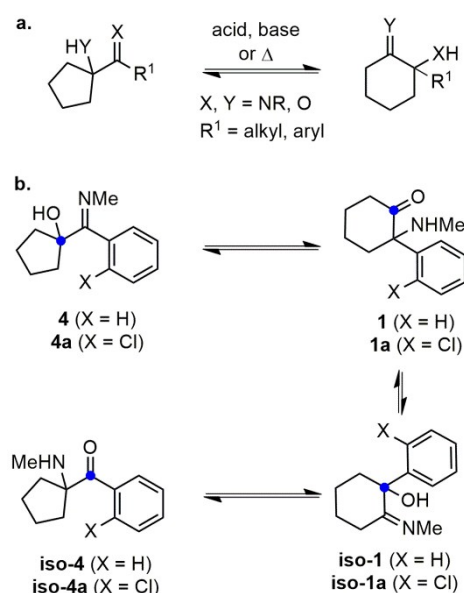

Fig. 8 a. General thermal rearrangement for α-ketols, α-iminols, α-aminoketones and α-aminoimines. **b.** Successive α-iminol/α-aminoketone rearrangements connecting iminol **4** to aminoketone **iso-4**. All these structures are isomers. Blue dots refer the same carbon among isomeric structures.

We first reproduced the original conditions reported by Stevens: the thermolysis of **4a** in the presence of 1 equiv. of HCl in dichlorobenzene at 180 °C gave (±)-**1a·HCl** in 74% yield after 30 min. When HCl was omitted, ketamine could not be extracted from the reaction mixture. Further screening of conditions for the thermolysis of **4a** and preliminary optimization were carried out in batch trials under microwave irradiation (see Supporting Information, Table S14).[17,44] For the sake of process simplification, ethanol was selected as solvent for the thermolysis of hydroxyimine **4a**. Although the addition of HCl was recommended by Stevens, its utilization led to two main issues: (a) a significant amount of ketone **7** was formed through the hydrolysis of hydroxyimine **4a**, and (b) the flow

setup required specific adaptations for high temperature and pressure operation in the presence of a strong acid. Preliminary trials under microfluidic conditions using PFA fluidic assemblies rapidly showed their limitations and were not compatible with process conditions involving temperatures > 180 °C and pressures > 15 bar. We thus changed the PFA microfluidic setups to SS microfluidic setups to improve the mechanical resistance under heat and pressure stresses, although this definitively excluded HCl as a coreagent.

Preliminary trials indicated that the thermal rearrangement of hydroxyimine **4a** requires at least 180 °C and 25 min of residence time to reach a conversion of 83%. (±)-**1a** could be isolated in 30% yield after recrystallization (Figure 9a). Prolonged reaction time at 180 °C or higher temperatures led to significant decomposition.

By contrast, exposure to high temperature at shorter residence times provided much cleaner reaction profiles with conversion of up to 80% (Table 4, entry 16) and up to 58% yield (77% selectivity, Table 4, entry 14) in (±)-**1a** (see Supporting Information, Table S16).
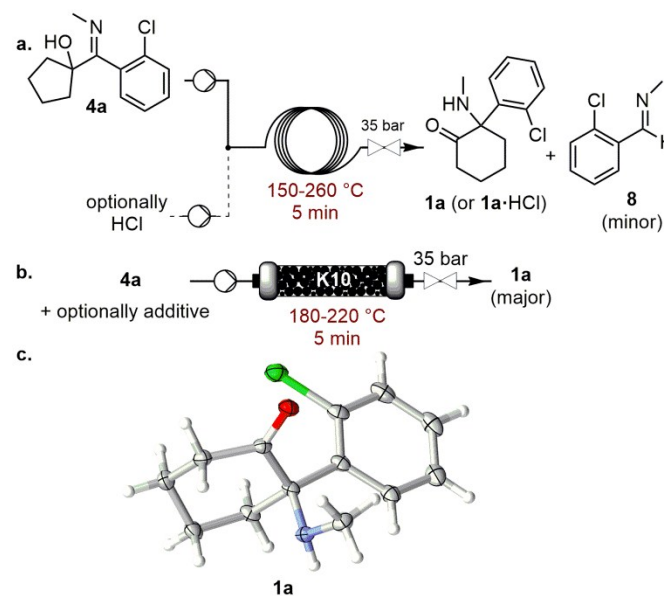
Fig. 9. a. Homogeneous thermolysis of iminol **4a** under microfluidic conditions under neutral or acid-catalyzed conditions (the cooling loop is omitted for clarity). **b.** Thermolysis of **4a** in the presence of Montmorillonite K10 as heterogeneous catalyst under flow conditions (the pre-heating and cooling loops are omitted for clarity). **c.** Molecular structure by single crystal X-ray diffraction analysis of free base (±)-**1a**. Only one molecule of the asymmetric unit is shown (See Supporting Information 2.8.2.3).

Table 4. Process optimization for the thermal rearrangement of α-iminol **4a** into (±)-**1a** free base under homogeneous conditions without HCl or additives.

Entry[a]	solvent	T (°C)	Conv. (%)[b]	Selec. for 1a (%)[b]	Selec. for 8 (%)[b]
1	EtOH	200	66	80	12
2[c]	EtOH	200	63	84	10
3	[EMIM][ES]	200	33	61	4
4	DMSO	200	10	60	39
5	MeTHF	200	7	26	73
6	toluene	200	15	27	45
7	EtOH	220	62	75	18
8[c]	EtOH	220	71	78	15
9	[EMIM][ES]	220	78	38	2
10	DMSO	220	59	56	38
11	MeTHF	220	17	29	70
12	toluene	220	31	28	45
13	EtOH	240	71	81	15
14[c]	EtOH	240	75	77	12
15	[EMIM][ES]	240	n.d.[d]	n.d.[d]	n.d.[d]
16	DMSO	240	80	45	50
17	MeTHF	240	40	29	62
18	toluene	240	47	34	28

[EMIM][ES] = ethylmethylimidazolium ethylsulfate. [a] Typical conditions: [**4a**] = 0.1 M; residence time = 5 min; P = 35 bar. [b] Conversion and selectivity were determined by HPLC/DAD processed at 216 nm. [c] [**4a**] = 0.42 M. [d] Complex HPLC chromatogram.

A small library of solvents with either low toxicity or considered as sustainable alternatives, as well as more conventional reaction media[30,31,33,45] (listed by increasing polarity: toluene, 2-methyltetrahydrofuran, ethanol, ethylmethylimidazolium ethylsulfate [EMIM][ES] and dimethylsulfoxide) was screened at temperatures ranging between 200 and 240 °C (35 bar, 5 min of residence time). Above 180 °C, a fragmentation process leading to *N*-(2-chlorobenzylidene) methanamine (**8**) and cyclopentanone became significant (see Supporting Information, Table S16).[13,14] The fragmentation process is favored in apolar solvents (toluene and MeTHF) and is inhibited in [EMIM][ES] and ethanol. The formation of hydroxyketone **7** in up to 10%, as well as other unidentified side-products was however observed in [EMIM][ES]. The cleanest reaction profiles with the highest conversion were obtained in ethanol in the 200-240 °C range (5 min of residence time, 35 bar), regardless of the concentration of **4a** (0.1 or 0.42 M, Table 4 and Supporting Information, Tables S16 and S17).

Since α-ketol and α-iminol rearrangements can also be promoted by Lewis acids,[41,46] homogeneous Lewis acids compatible with the upstream operations were screened (Table 5). In particular, (Ti(O*i*Pr)₄) or B(O*i*Pr)₃ were were investigated as homogeneous co-additives (2 equiv.) in the feed solution of **4a** (0.1 M in ethanol). While Ti(O*i*Pr)₄ prevented the rearrangement of **4a** to occur and yielded complex reaction profiles in the 200-240 °C range, B(O*i*Pr)₃ somehow inhibited the reaction at 200 °C, but gave similar results at 220 °C as entry 7 in Table 4 (no additives). These

Table 5. Process optimization for the thermal rearrangement of α-iminol **4a** into (±)-**1a** (free base) under homogeneous conditions in the presence of 2 equivalents of Lewis acids.

Entry[a]	additive	T (°C)	Conv. (%)[b]	Selec. for 1a (%)[b]	Selec. for 8 (%)
1	Ti(O*i*Pr)₄	200	16	78	12
2	B(O*i*Pr)₃	200	10	74	8
3	Ti(O*i*Pr)₄	220	33	48	12
4	B(O*i*Pr)₃	220	61	81	14
5	Ti(O*i*Pr)₄	240	33	24	15
6	B(O*i*Pr)₃	240	76	58	39

[a] Conditions: solvent = EtOH; [**4a**] = 0.1 M; [additive] = 0.2 M; residence time = 5 min; P = 35 bar. [b] Conversion and selectivity were determined by HPLC/DAD processed at 216 nm.

results are thus very encouraging for the perspectives of process concatenation (see below), although no activation effect could be emphasized with such homogeneous Lewis acids.

Clays and silica can also be used to promote the rearrangement of α-ketols and α-iminols.[41,47] In particular, Montmorillonite K10 is a well-studied solid heterogeneous acid catalyst.[48] Preliminary trials in vials under microwave irradiation (see Supporting Information, Table S15) gave very promising results, with short reaction times, high conversion and selectivity in the presence of Montmorillonite K10. These results were next transposed under continuous flow conditions. The microfluidic setup consisted of a SS packed-bed reactor filled with 3.7 g of Montmorillonite K10 connected upstream to a HPLC pump for delivering the liquid feed at 0.8-1.6 mL min⁻¹ flow rates. The packed-bed reactor was inserted in a thermoregulated oven, and backpressure regulation was included downstream (Figure 9b). Samples were taken periodically from the reactor effluents, and no deactivation of the catalyst could be evidenced upon processing 50 mL of feedstock solution. Several solvents were assessed as well, and ethanol gave the best results (Table 6 and Supporting Information, Table S17). The reaction is dramatically enhanced in the presence of Montmorillonite K10, even using solvents that were not favorable under homogeneous conditions, such as 2-methyltetrahydrofuran and toluene. High conversion (75%) and selectivity (95%) were obtained at 180 °C, under 35 bar of counter-pressure in ethanol, with a 0.1 M feedstock solution of **4a** that was delivered at 1.6 mL min⁻¹ (entry 1). The HPLC trace of the reactor effluent was very clean, showing essentially (±)-**1a** and unreacted **4a** (see Supporting Information, Figure S27). The influence of 2 equiv. of B(O*i*Pr)₃ on the reaction was also evaluated in the 180-220 °C range in ethanol. Identical results as for the additive-free experiments were obtained (see Supporting Information, Table S17).

Eventually, experiments were carried out at 180 °C with a more concentrated feedstock solution of **4a** (0.42 M in EtOH). Higher concentrations led to a decrease in conversion from 75 (0.1 M) to 57% (0.42 M) with a flow rate of 1.6 mL min⁻¹

ARTICLE

Journal Name

Table 6. Process optimization for the thermal rearrangement of α-iminol **4a** into (±)-**1a** (free base) under heterogeneous conditions.

| Entry[a]	solvent	T (°C)	Conv. (%)[b]	Selec. for 1a (%)[b]	Selec. for 8 (%)[b]
1	EtOH	180	75	95	<1
2[c]	EtOH	180	57	91	<1
3[c,d]	EtOH	180	69	89	<1
4	[EMIM][ES]	180	26	94	<1
5	DMSO	180	16	69	9
6	MeTHF	180	73	89	<1
7	toluene	180	75	92	<1
8	EtOH	200	75	91	<1
9	[EMIM][ES]	200	40	85	<1
10	DMSO	200	30	69	12
11	MeTHF	200	73	81	<1
12	toluene	200	78	68	5

[EMIM][ES] = ethylmethylimidazolium ethylsulfate. [a] Typical conditions: [**4a**] = 0.1 M; flow rate = 1.6 mL min^{-1}; P = 35 bar; 3.7 g of Montmorillonite K10 in the packed-bed. [b] Conversion and selectivity were determined after injection of 50 mL of feedstock solution through the packed-bed, by HPLC/DAD processed at 216 nm. [c] [**4a**] = 0.42 M. [d] flow rate = 0.8 mL min^{-1}.

(entries 1-2). This behavior was quite expected, as the availability of the active sites on the catalyst decreases with the concentration of the feedstock solution. Decreasing the flow rate to 0.8 mL min^{-1} helped to restore the conversion (69%) while maintaining a high selectivity (89%) for (±)-**1a** (entry 3). Upon concentration and cooling of the reactor effluent, (±)-**1a** crystallized and could be recovered by simple filtration (36% isolated yield, 99% purity). The concentrated mother liquor containing unreacted α-iminol **4a** could be recycled for further thermolysis, thus enabling a daily productivity of 71 g for (±)-**1a** (free base). Alternatively, (±)-**1a**·HCl could be collected directly by slow addition of a solution of hydrochloric acid in diethyl ether to the crude reactor effluent (62% isolated yield, 99% conversion).

The complexity of the thermal isomerization of hydroxyimine **4a** arises mainly from the emergence of interconnected equilibria that relate the 4 structural isomers of (±)-**1a**, in addition to other competitive processes including hydrolysis, fragmentation and other decomposition reactions. DFT computations were undertaken on the unimolecular rearrangement of α-iminol **4a** toward (±)-**1a** considering basic (anionic), neutral and acidic (cationic) conditions (Figure 10) for gathering mechanistic information. Thermochemistry computations indicated that the ring expansion from **4a** to (±)-**1a** is an endergonic reaction (see Supporting Information, sections 3.2 and 3.3), and it critically depends on the conditions: $\Delta G°_{an}$ = 13.8 kcal mol^{-1}, $\Delta G°_{neut}$ = 4.4 kcal mol^{-1} and $\Delta G°_{cat}$ = 26.5 kcal mol^{-1}. The corresponding transition states are structurally related to those identified for the α-ketol rearrangement (see Figure 5). The activation barrier is less sensitive to the presence of a base than for the α-ketol rearrangement. The anionic pathway, thus involving the conjugated base of **4a** (*i.e.* a thermal rearrangement in the presence of a base), gave the lowest activation barrier ($\Delta G^{\ddagger}_{an}$ =

23.3 kcal mol^{-1}), followed with the neutral pathway ($\Delta G^{\ddagger}_{neut}$ = 31.6 kcal mol^{-1}) and the cationic pathway (*i.e.* a thermal rearrangement in the presence of a Brønsted acid, $\Delta G^{\ddagger}_{cat}$ = 31.9 kcal mol^{-1}). The experimental data collected upon preliminary optimization showed that the addition of a Brønsted base or a Brønsted acid led to complex reaction profiles, despite the formation of (±)-**1a**. The addition of Lewis acids of increasing strength did not lead to a decrease of the activation barrier, in agreement with our experimental results: in the presence of boron trifluoride or boron trimethoxide, the computed activation barriers were of 36.4 and 36.0 kcal mol^{-1}, respectively.

The entire reaction profile connecting the four isomers of ketamine is depicted in Figure 10 (see Supporting Information, sections 3.1-3.5 for details). Computations emphasized that these rearrangements proceed through unimolecular processes with rather high activation barriers. Once formed, ketamine (±)-**1a** can further isomerize through a concerted asynchronous migration of the phenyl group leading to its cyclohexyliminol isomer **iso-1a**. The thermal isomerization of (±)-**1a** to **iso-1a** has an activation barrier of 27.9 kcal mol^{-1}, which is *ca.* 3.7 kcal mol^{-1} below the thermal isomerization of **4a** to (±)-**1a**. Compound **iso-1a** can next undergo a ring contraction through a similar mechanism as for the isomerisation of **4a** to (±)-**1a**, leading to aminoketone **iso-4a** yet with a smaller activation barrier (22.9 kcal mol^{-1}). These computations thus corroborate Stevens' conclusions in the sense that the most straightforward chemical route to prepare ketamine starts from α-iminol **4a** rather than from aminoketone **iso-4a**. Both kinetic and thermodynamic data from these thermochemistry computations also emphasize the complexity of the process, and the difficulty to achieve high conversion and selectivity for the formation of (±)-**1a**. The unfavorable position of the equilibrium between **4a** and (±)-**1a**, as well as the high activation barriers and low $\Delta\Delta G^{\ddagger}$ between the competitive reactions are only a few elements underneath such complexity. Similar trends were obtained for other structurally related compounds, such as the precursors of norketamine and *N*-benzylnorketamine (±)-**1b,c**, respectively (see Supporting Information, section 3.2).
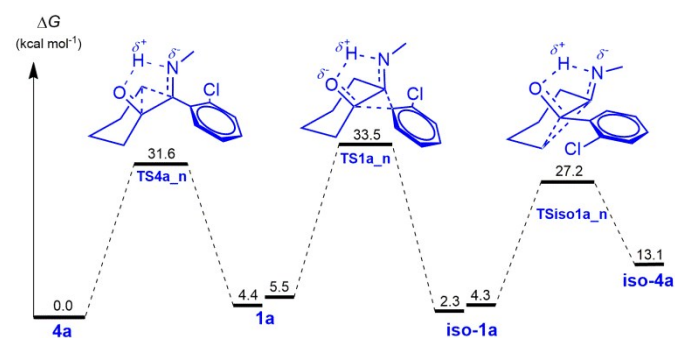
Fig. 10. Transition state structures and relative Gibbs free energy (ΔG) for the thermal isomerization of **4a** under neutral conditions.

Concatenation of the individual steps under microfluidic conditions and preparation of ketamine and analogs

The concatenation of steps 1-2 was rather straightforward upon minor adjustments for the hydroxylation and the imination steps (Figure 11). For the hydroxylation step, additive PEG-400 was set at 50 mol% in the feedstock solution to reduce the viscosity. Upon optimization of the imination step from hydroxyketone 7, the best conditions involved a slight excess of methylamine (1.5 equiv.) in the presence of B(O*i*Pr)$_3$ (2 equiv.) at 60 °C (1 min of residence time, Table 3). However, upon direct concatenation with the hydroxylation step, significant amounts of isomeric hydroxyketone **iso-7** (26%) were detected along with hydroxyimine **4a**. The formation of isomeric **iso-7** can be easily rationalized: the combination of a higher temperature for the imination step (60 °C) and the presence of residual KOH from the hydroxylation step likely favors the competitive α-ketol isomerization of **7** to **iso-7** (see above). An obvious solution was therefore to decrease the temperature for the imination step (25 °C), combined with an increase of the residence time (2 min). Under such conditions, compound **4a** was obtained in 98% conversion and 95% selectivity.

By changing Feed 2 from methylamine to ammonia or benzylamine, iminols **4b,c** were obtained as precursors of norketamine (±)-**1b** and *N*-benzylnorketamine (±)-**1c**. The imination of **7** with ammonia gave iminol **4b** with a lower conversion (55%) but with excellent selectivity (98%) regardless of the excess of ammonia, while the imination with benzylamine proceeded extremely well with 99% conversion and selectivity. The reactor effluent from the concatenated hydroxylation-imination steps was collected in a surge, and diluted with ethanol prior thermolysis.
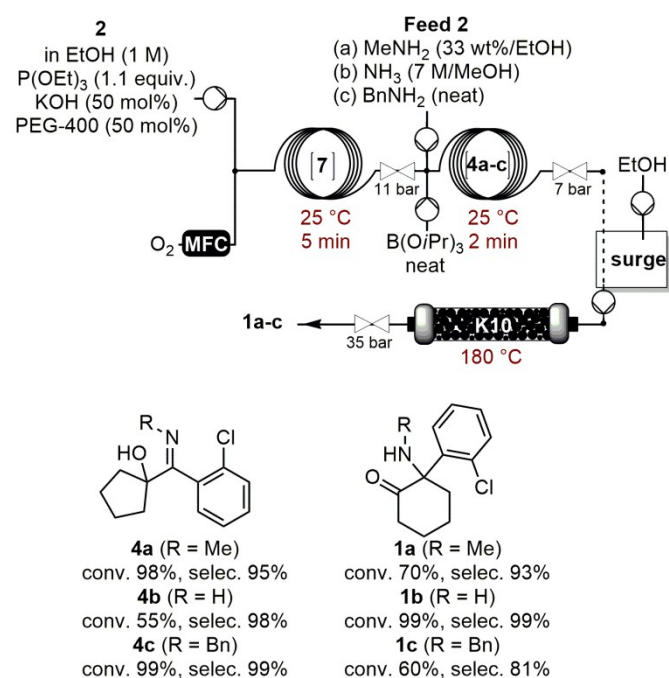
The direct concatenation toward the thermolysis of iminols **4a-c** was attempted, and the reactor effluent from the imination step was reacted in a packed-bed reactor filled with Montmorillonite K10 operated at 180 °C (35 bar). Good conversion and selectivity ((±)-**1a**: conv. (**4a**) = 70%, selec. 93%; (±)-**1b**: conv. (**4b**) = 99%, selec. 99% or (±)-**1c**: conv. (**4b**): 60%, selec. 81%) were maintained for 20 min, but then rapidly decreased. The deactivation of the catalyst is likely due to residual potassium hydroxide from the hydroxylation step or amines from the imination step, which would eventually poison acidic sites of K10.

Upon collection of the final reactor effluent containing ketamine, triethyl phosphate, PEG-400 and the excess triisopropyl borate remained in the mother liquor regardless of the isolation procedure (cooling crystallization to get ketamine free base or reactive crystallization with HCl in diethyl ether to get ketamine hydrochloride). No attempts for recycling triethyl phosphate, PEG-400 or triisopropyl borate were made. The mother liquor was then handled as a non-halogenated organic waste, and disposed through the EH&S Department.

Conclusion

This work illustrates an economically and environmentally favorable alternative for the preparation of active pharmaceutical ingredient ketamine that bypasses problematic steps or conditions. It provides concrete, atom economic and robust conditions for the continuous flow preparation of ketamine. The procedure relies on the main assets of continuous processing and utilizes exclusively low toxicity reagents and a FDA class 3 solvent (ethanol) under intensified conditions. The procedure is amenable to the production of ketamine analogs, being of paramount importance within the current pharmaceutical perspectives for new potent antidepressant medications.

Starting from a commercially available ketone (that can also be synthesized from cheap, widely and available chemicals), this flow process features three steps including (a) a unique continuous flow hydroxylation procedure step relying on molecular oxygen in the presence of a substoichiometric amount of potassium hydroxide and PEG-400, (b) a fast imination with methylamine (1.5 equiv.) relying on triisopropyl borate (2 equiv.) and (c) a thermolysis relying on Montmorillonite K10 as a heterogeneous catalyst. Each step can be run independently, or can be concatenated within one single uninterrupted reactor network, while keeping high productivity with a minimal footprint. Ketamine free base can be directly crystallized from ethanol upon concentration of the thermolysis reactor effluent, affording 36% isolated yield (99% purity). Alternatively, (±)-**1a**·HCl can be precipitated in 62% isolated yield (99% purity) upon addition of HCl in diethyl ether to the effluent of the reactor. The most critical optimizations were supported by a computational study that provided insights on mechanisms and selectivity, and hence concrete solutions to avoid the formation of undesirable side products. To further complement the study, the scalability of the critical

Fig. 11. Concatenation toward racemic ketamine and analogs (±)-**1a-c**.

hydroxylation step was assessed in a pilot continuous mesofluidic reactor.

Conflicts of interest

There are no conflicts to declare.

Acknowledgments

Notes and *references*

1   M. W. Tyler, H. B. Yourish, D. F. Ionescu and S. J. Haggarty, *ACS Chem. Neurosci.*, 2017, **8**, 1122–1134.

2   World Health Organization, *WHO Model List of Essential Medicines - 20th List*, 2017, http://www.who.int/medicines/publications/essentialmedicines/en/ (Accessed January 19, 2019).

3   U. S. Drug Enforcement Administration, *The Controlled Substances Act,* https://www.dea.gov/controlled-substances-act (Accessed January 19, 2019).

4   The Center for Integrated Technology and Organic Synthesis (CiTOS) is licensed for the manufacturing of ketamine by the Federal Agency of Medicine and Health Products (License #620029).

5   Y. Yang, Y. Cui, K. Sang, Y. Dong, Z. Ni, S. Ma and H. Hu, *Nature*, 2018, **554**, 317–322.

6   World Health Organization, *Mental Health,* https://www.who.int/mental_health/management/depression/en/ (Accessed January 19, 2019).

7   U. S. National Library of Medicine, *A Study to Evaluate the Efficacy, Pharmacokinetics, Safety and Tolerability of Flexible Doses of Intranasal Esketamine Plus an Oral Antidepressant in Adult Participants With Treatment-resistant Depression,* https://clinicaltrials.gov/ct2/show/NCT03434041 (Accessed January 19, 2019).

8   P. Zanos, R. Moaddel, P. J. Morris, P. Georgiou, J. Fischell, G. I. Elmer, M. Alkondon, P. Yuan, H. J. Pribut, N. S. Singh, K. S. S. Dossou, Y. Fang, X.-P. Huang, C. L. Mayo, I. W. Wainer, E. X. Albuquerque, S. M. Thompson, C. J. Thomas, C. A. Zarate Jr and T. D. Gould, *Nature*, 2016, **533**, 481–486.

9   C. L. Stevens, R. D. Elliott and B. L. Winch, *J. Am. Chem. Soc.*, 1963, **85**, 1464–1470.

10   C. L. Stevens, A. Thuillier and F. A. Daniher, *J. Org. Chem.*,

1965, **30**, 2962–2966.

11   C. L. Stevens, I. L. Klundt, M. E. Munk and M. D. Pillai, *J. Org. Chem.*, 1965, **30**, 2967–2972.

12   C. L. Stevens, H. T. Hanson and K. G. Taylor, *J. Am. Chem. Soc.*, 1966, **88**, 2769–2774.

13   C. L. Stevens, A. B. Ash, A. Thuillier, J. H. Amin, A. Balys, W. E. Dennis, J. P. Dickerson, R. P. Glinski, H. T. Hanson, M. D. Pillai and J. W. Stoddard, *J. Org. Chem.*, 1966, **31**, 2593–2601.

14   C. L. Stevens, A. Thuillier, K. G. Taylor, F. A. Daniher, J. P. Dickerson, H. T. Hanson, N. A. Nielsen, N. A. Tikotkar and R. M. Weier, *J. Org. Chem.*, 1966, **31**, 2601–2607.

15   C. L. Stevens, F. E. Glenn and P. M. Pillai, *J. Am. Chem. Soc.*, 1973, **95**, 6301–6308.

16   L. Chen, Y. Gong and R. Salter, *J. Label. Compd. Radiopharm.*, 2018, **61**, 864–868.

17   P. J. Morris, R. Moaddel, P. Zanos, C. E. Moore, T. Gould, C. A. Zarate Jr. and C. J. Thomas, *Org. Lett.*, 2017, **19**, 4572–4575.

18   S. A. Chambers, J. M. DeSousa, E. D. Huseman and S. D. Townsend, *ACS Chem. Neurosci.*, 2018, **9**, 2307–2330.

19   Z.-Q. Zhang, T. Chen and F.-M. Zhang, *Org. Lett.*, 2017, **19**, 1124–1127.

20   R. Yokoyama, S. Matsumoto, S. Nomura, T. Higaki, T. Yokoyama and S.-I. Kiyooka, *Tetrahedron*, 2009, **65**, 5181–5191.

21   X. Yang and F. D. Toste, *J. Am. Chem. Soc.*, 2015, **137**, 3205–3208.

22   K. Steiner, S. Gangkofner, J.-M. Grunenwald, US Pat. 6040479, 2000.

23   R. Gérardy, N. Emmanuel, T. Toupy, V.-E. Kassin, N. N. Tshibalonza, M. Schmitz and J.-C. M. Monbaliu, *Eur. J. Org. Chem.*, 2018, 2301–2351.

24   R. Gérardy and J.-C. M. Monbaliu, *Multistep Continuous-Flow Processes for the Preparation of Heterocyclic Active Pharmaceutical Ingredients* in *Topics in Heterocyclic Chemistry: Flow Chemistry for the Synthesis of Heterocycles*, eds. U. K. Sharma and E. V. Van der Eycken, Springer International Publishing, Cham, 2018, pp. 1–102.

25   M. J. Frisch, G. W. Trucks, H. B. Schlegel, G. E. Scuseria, M. A. Robb, J. R. Cheeseman, G. Scalmani, V. Barone, B. Mennucci, G. A. Petersson, H. Nakatsuji, M. Caricato, X. Li, H. P. Hratchian, A. F. Izmaylov, J. Bloino, G. Zheng, J. L. Sonnenberg, M. Hada, M. Ehara, K. Toyota, R. Fukuda, J. Hasegawa, M. Ishida, T. Nakajima, Y. Honda, O. Kitao, H. Nakai, T. Vreven, J. A. Montgomery Jr, J. E. Peralta, F. Ogliaro, M. Bearpark, J. J. Heyd, E. Brothers, K. N. Kudin, V. N. Staroverov, R. Kobayashi, J. Normand, K. Raghavachari, A. Rendell, J. C. Burant, S. S. Iyengar, J. Tomasi, M. Cossi, N. Rega, J. M. Millam, M. Klene, J. E. Knox, J. B. Cross, V. Bakken, C. Adamo, J. Jaramillo, R. Gomperts, R. E. Stratmann, O. Yazyev, A. J. Austin, R. Cammi, C. Pomelli, J. W. Ochterski, R. L. Martin, K. Morokuma, V. G. Zakrzewski, G. A. Voth, P. Salvador, J. J. Dannenberg, S. Dapprich, A. D. Daniels, Ö. Farkas, J. B. Foresman, J. V. Ortiz, J. Cioslowski and D. J. Fox, *Gaussian 09 (Revision D.01),* Gaussian Inc., Wallingford CT, 2009.

View Article Online
DOI: 10.1039/C9GC00376G

26   C. A. Hone and C. O. Kappe, *Top. Curr. Chem.*, 2019, **377**, 2.

27   Y.-F. Liang and N. Jiao, *Angew. Chem. Int. Ed.*, 2014, **53**, 548–552.

28   S.-B. D. Sim, M. Wang and Y. Zhao, *ACS Catal.*, 2015, **5**, 3609–3612.

29   M. B. Chaudhari, Y. Sutar, S. Malpathak, A. Hazra and B. Gnanaprakasam, *Org. Lett.*, 2017, **19**, 3628–3631.

30   R. K. Henderson, C. Jiménez-González, D. J. C. Constable, S. R. Alston, G. G. A. Inglis, G. Fisher, J. Sherwood, S. P. Binks and A. D. Curzons, *Green Chem.*, 2011, **13**, 854–862.

31   D. Prat, O. Pardigon, H.-W. Flemming, S. Letestu, V. Ducandas, P. Isnard, E. Guntrum, T. Senac, S. Ruisseau, P. Cruciani and P. Hosek, *Org. Process Res. Dev.*, 2013, **17**, 1517–1525.

32   F. P. Byrne, S. Jin, G. Paggiola, T. H. M. Petchey, J. H. Clark, T. J. Farmer, A. J. Hunt, C. R. McElroy and J. Sherwood, *Sustain. Chem. Process.*, 2016, **4**, 7.

33   D. Prat, A. Wells, J. Hayler, H. Sneddon, C. R. McElroy, S. Abou-Shehada and P. J. Dunn, *Green Chem.*, 2016, **18**, 288–296.

34   C. Mendoza, N. Emmanuel, C. A. Páez, L. Dreesen, J.-C. M. Monbaliu and B. Heinrichs, *ChemPhotoChem*, 2018, **2**, 890–897.

35   S. Isayama, *Bull. Chem. Soc. Jpn.*, 1990, **63**, 1305–1310.

36   The H412 hazard statement for triethylphosphite (MSDS) indicates potential harm to aquatic life with a lasting effect. However, the procedure developed in this manuscript requires a very slight excess of P(OEt)$_3$ (1.1 equiv.) that is oxidized into triethyl phosphate under the reaction conditions. Triethyl phosphate is a non-toxic substance according to its MSDS.

37   E. Weber, *Crown Ethers* in *Ullmann's Encyclopedia of Industrial Chemistry*, Wiley-VCH Verlag GmbH & Co. KGaA, Weinheim, Germany, 2007, DOI: 10.1002/14356007.a08_091.pub2.

38   C. L. Stevens, T. A. Treat and P. M. Pillai, *J. Org. Chem.*, 1972, **37**, 2091–2097.

39   M. T. Sabatini, L. T. Boulton and T. D. Sheppard, *Sci. Adv.*, 2017, **3**, e1701028.

40   J. T. Reeves, M. D. Visco, M. A. Marsini, N. Grinberg, C. A. Busacca, A. E. Mattson and C. H. Senanayake, *Org. Lett.*, 2015, **17**, 2442–2445.

41   L. A. Paquette and J. E. Hofferberth, *The α-Hydroxy Ketone (α-Ketol) and Related Rearrangements* in *Organic Reactions*, John Wiley & Sons, Inc., Hoboken, NJ, USA, 2004, DOI: 10.1002/0471264180.or062.03.

42   J. Jose, S. A. Gamage, M. G. Harvey, L. J. Voss, J. W. Sleigh and W. A. Denny, *Bioorg. Med. Chem.*, 2013, **21**, 5098–5106.

43   H. Elhawi, H. Eini, A. Douvdevani and G. Byk, *Molecules*, 2012, **17**, 6784–6807.

44   T. N. Glasnov and C. O. Kappe, *Chem. Eur. J.*, 2011, **17**, 11956–11968.

45   J. P. Hallett and T. Welton, *Chem. Rev.*, 2011, **111**, 3508–3576.

46   X. Zhang, R. J. Staples, A. L. Rheingold and W. D. Wulff, *J. Am. Chem. Soc.*, 2014, **136**, 13971–13974.

47   X. Zhang, Y. Dai and W. D. Wulff, *Synlett*, 2018, **29**, 2015–2018.

48   M. Hechelski, A. Ghinet, B. Louvel, P. Dufrénoy, B. Rigo, A. Daïch and C. Waterlot, *ChemSusChem*, 2018, **11**, 1249–1277.

View Article Online
DOI: 10.1039/C9GC00336C

Green Chemistry Accepted Manuscript